Direct EPR Spectroscopic Evidence for an Allylic Radical Generated from (*E*)-2′-Fluoromethylene-2′-deoxycytidine 5′-Diphosphate by *E. coli* Ribonucleotide Reductase

Wilfred A. van der Donk,[†] Gary J. Gerfen,[¥] and JoAnne Stubbe*

Departments of Chemistry and Biology
Massachusetts Institute of Technology
Cambridge, Massachusetts 02139

Received November 26, 1997

(*E*)-2′-Fluoromethylene-2′-deoxycytidine, (*E*)-FMC, has potent antiproliferative activity against a wide range of tumor cell lines.[1] Its cytotoxicity is thought to arise from a synergistic effect between its triphosphate, a DNA chain terminator,[1] and its diphosphate (FMCDP), a stoichiometric inactivator of ribonucleotide reductase (RNR).[2] RNRs catalyze the conversion of nucleotides to deoxynucleotides, the rate-determining step in DNA biosynthesis. The class I RNRs are composed of two subunits: R1 and R2. Initiation of the reduction process is thought to proceed via a thiyl radical on R1 abstracting the 3′-hydrogen atom from the nucleotide. While much indirect evidence supports this proposal, direct evidence for a 3′-nucleotide radical intermediate has been elusive. Our recent studies indicate that FMCDP is a mechanism-based inhibitor of RNR. The inactivation is accompanied by loss of fluoride ion, stoichiometric alkylation of the R1 subunit, loss of the essential tyrosyl radical (Y•) on the R2 subunit, and formation of a new nucleotide-based radical.[2b,c] To establish the structure of this radical, [6′-^{13}C]-(*E*)-FMCDP was synthesized and incubated with RNR. EPR studies of the resulting radical establish that it is allylic, requiring that RNR catalyzes 3′-hydrogen atom abstraction.

On the basis of biochemical and EPR data, two mechanisms for nucleotide radical generation from FMCDP have been proposed.[2c] The initial step in both is 3′-hydrogen atom abstraction to generate a fluorinated allyl radical (Scheme 1). This radical can be reduced by hydrogen atom transfer from one of the three cysteine residues in the active site. Reduction from the α-face or the *β*-face of the nucleotide (pathways A and B, respectively), followed by loss of fluoride ion, results in the generation of **1** and a cysteinyl radical. In pathway A, Glu441 adds to the exocyclic methylene of **1** to generate **2** which is converted to allyl radical **3** via hydrogen atom abstraction by a thiyl radical on the α-face of the nucleotide. In pathway B, the thiyl radical of Cys439 adds directly to **1**, resulting in formation of the ketyl radical **4**. A distinction between these two mechanistic possibilities could not be made unambiguously; however, the allyl radical pathway A was favored on the basis of simulations of 9 and 140 GHz EPR data from [6′-^{2}H]- and [6′-^{1}H]-(*E*)-FMCDP.[2c]

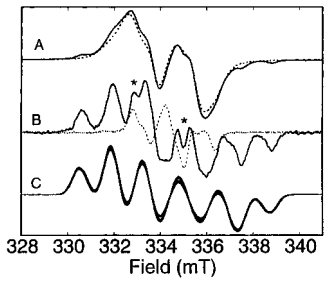

Figure 1. (A) 9.39 GHz EPR spectrum of a sample containing RNR (50 *μ*M), [6′-^{13}C]-(*E*)-FMCDP (0.5 mM), and ATP (1.6 mM) frozen 30 s after addition of the inhibitor (solid line) overlayed with the spectrum of Y122• (- - -). The intensity of the Y• signal was normalized to reflect the radical concentration at $t = 30$ s as quantitated by the absorbance at 410 nm.[2c] (B) New radical signal at $t = 30$ s after subtraction of the Y122• signal. Instrument settings: power 10 *μ*W, modulation amplitude 0.39 mT, $T = 109$ K. The overlaid (···) spectrum derives from [6′-^{12}C]-(*E*)-FMCDP, showing that the peaks marked with an asterisk most likely arise from residual unlabeled material. (C) Family of 10 best-fit simulations of the [6′-^{13}C] spectrum using the parameter set given in Table 1.

Table 1. Hyperfine Values for the ^{13}C-Labeled Radical As Determined by the Simulations in Figure 1C[a]

	H^{α}	H^{β}	^{13}C
A_1	2.1(0.2)	1.3(0.3)	1.1(0.4)
A_2	0.7(0.3)	1.4(0.3)	0.2(0.3)
A_3	1.4(0.3)	1.4(0.3)	5.5(0.2)
A_{iso}	1.4(0.3)	1.4(0.3)	2.3(0.2)

[a] The numbers in parentheses are estimated uncertainties. $g_1 = 2.0030$, $g_2 = 2.0042$, and $g_3 = 2.0018$. For principal axis orientations, see ref 9.

To establish the structure of the radial, [6′-^{13}C]-(*E*)-FMCDP was synthesized on the basis of the route developed by McCarthy and co-workers[3] starting with the [^{13}C]-methylation of thiophenol (Scheme 2).[2b,4−7] [6′-13C]-(*E*)-FMCDP was obtained, and the NMR analysis indicated 96−97% ^{13}C-incorporation into 6′-C (Supporting Information).

[6′-^{13}C]-(*E*)-FMCDP was incubated with *E. coli* RNR, and after 30 s the sample was frozen in liquid N_2, and the EPR spectrum was recorded at 9.39 GHz. The resulting spectrum is shown in Figure 1A overlayed with the spectrum of Y•. Subtraction of 0.82 equiv of Y• signal gave rise to the signal shown in Figure 1B. Spin quantitation revealed 0.14 equiv of new radical/equiv of RNR.[2c] Since the ^{13}C-labeled nucleotide contains 3−4% of ^{12}C-labeled material, a minor component of the signal is derived from unlabeled radical (Figure 1B).

To establish the structure of this radical, simulations were generated using a simulated annealing protocol[8] (see the Supporting Information). Proton hyperfine parameters and *g*-values

* Corresponding author. Phone: (617) 253-1814. Fax: (617) 258-7247. E-mail: stubbe@mit.edu.
[†] Present address: Department of Chemistry, University of Illinois at Urbana-Champaign, Urbana, IL 61801.
[‡] Present address: Department of Physiology and Biophysics, Albert Einstein College of Medicine of Yeshiva University, 1300 Morris Park Ave., Bronx, NY 10461.

(1) McCarthy, J. R.; Sunkara, P. S. In *Design, Synthesis and Antitumor Activity of an Inhibitor of Ribonucleotide Reductase*; McCarthy, J. R., Sunkara, P. S., Eds.; CRC Press: Boca Raton, FL, 1995; pp 3−32. (b) McCarthy, J.; Sunkara, P. S.; Matthews, D. P.; Bitonti, A. J.; Jarvi, E. T.; Sabol, J. S.; Resvick, R. J.; Huber, E. W.; van der Donk, W. A.; Yu, G.; Stubbe, J. *ACS Symp. Ser.* **1996**, *639*, 246−264 (c) Bitonti, A. J.; Dumont, J. A.; Bush, T. L.; Cashman, E. A.; Cross-Doersen, D. E.; Wright, P. S.; Matthews, D. P.; McCarthy, J. R.; Kaplan, D. A. *Cancer Res.* **1994**, *54*, 1485−1490. (d) Bitonti, A. J.; Bush, T. I.; Lewis, M. T.; Sunkara, P. S. *Anticancer Res.* **1995**, *15*, 1179−1182.

(2) (a) Sunkara, P. S.; Lippert, B. J.; Snyder, R. D.; Jarvi, E. T.; Farr, R. A. *Proc. Am. Assoc. Cancer Res.* **1988**, *29*, 324. (b) van der Donk, W. A.; Yu, G.; Silva, D. J.; Stubbe, J.; McCarthy, J. R.; Jarvi, E. T.; Matthews, D. P.; Resvick, R. J.; Wagner, E. *Biochemistry* **1996**, *35*, 8381−8391. (c) Gerfen, G. J.; van der Donk, W. A.; Yu, G.; McCarthy, J. R.; Matthews, D. P.; Jarvi, E. T.; Farrar, C.; Griffin, R. G.; Stubbe, J. *J. Am. Chem. Soc.*, in press.

(3) McCarthy, J. R.; Matthews, D. P.; Sabol, J. S.; McConnell, J. R.; Donaldson, R. E.; Duquid, R. US Patent 5,589,587, 1996.

(4) Ono, N.; Miyake, H.; Saito, T.; Kaji, A. *Synthesis* **1980**, 952−953.

(5) Johnson, C. R.; Keiser, J. E. *Org. Synth.* **1967**, *46*, 791−793.

(6) (a) McCarthy, J. R.; Matthews, D. P.; Paolini, J. P. *Org. Synth.* **1994**, *72*, 209−215. (b)Robins, M. J.; Wnuk, S. F. *J. Org. Chem.* **1993**, *58*, 3800−3801.

(7) (a) Yoshikawa, M.; Kato, T.; Takenishi, T. *Tetrahedron Lett.* **1967**, *50*, 5065−5068. (b) Hoard, D. E.; Ott, D. G. *J. Am. Chem. Soc.* **1965,** *87*, 1785−1788.

S0002-7863(97)04027-4 CCC: $15.00
Published on Web 04/22/1998

Scheme 1

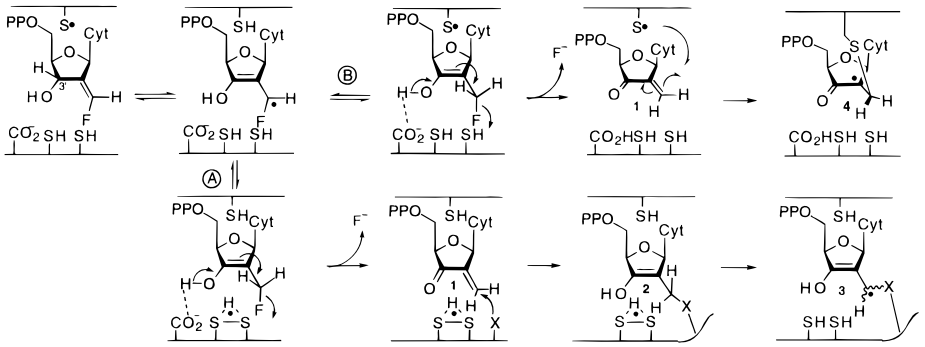

Scheme 2[a]

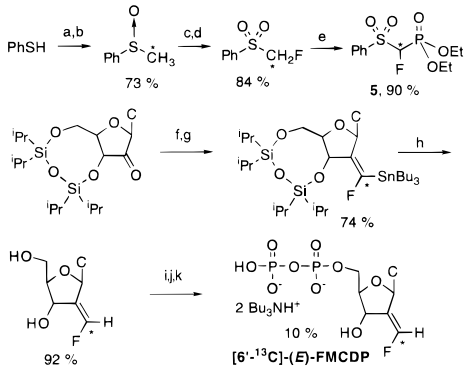

[a] Conditions: (a) $^{13}CH_3I$, DBU; (b) $NaIO_4$; (c) DAST, $SbCl_3$; (d) Oxone; (e) $ClP(O)(OEt)_2$, 2 equiv of LiHMDS; (f) **6**, KO^{t}Bu; (g) Bu_3SnH, AIBN; (h) CsF, MeOH; (i) $POCl_3$; (j) H_2O; (k) CDI, $Bu_3NH{\cdot}H_2PO_4$.

were constrained to those determined in our previous X- and D-band EPR studies,[2c] while ^{13}C principal values were allowed to vary between 0 and 2.5 mT (A_1 and A_2) and 4.0−6.5 mT (A_3).[9] The 10 best fit simulations are shown in Figure 1C.[9]

The measured isotropic ^{13}C hyperfine coupling of 2.3 mT (Table 1) yields a spin density on C6′ of 0.64,[10,11] which is very diagnostic for allyl radicals.[12] The isotropic hyperfine coupling value expected for a ketyl radical, **4**, has been reported as ∼1.0 mT,[13] which is well outside the uncertainty of our measured value. In addition g_{iso} is 2.003, also outside the range for reported ketyl radicals. Thus, the ^{13}C hyperfines and the excellent simulations unambiguously establish that the radical signal derived from FMCDP is allylic in nature and lacks a fluorine. This structure can only be generated by removal of the hydrogen atom from C3′ of FMCDP. Thus, direct evidence for a nucleotide radical and the importance to 3′ chemistry in its formation is provided.

Acknowledgment. This work was supported by a grant from the National Institutes of Health to J.S. (GM-29595) and by a fellowship from the Jane Coffin Childs Fund to W.A.v.d.D. (Project 61-960). We thank Drs. J. R. McCarthy and R. E. Richardson for advice on the preparation of [6′-^{13}C]-(*E*)-FMCDP.

Supporting Information Available: ^1H and ^{31}P NMR spectra for (*E*)-FMCMP, a table of changes in the previously reported NMR data for compounds shown in Scheme 2 that are due to the introduction of a ^{13}C-label, and full details of the simulated annealing protocol (3 pages, print/PDF). See any current masthead page for ordering information and Web access instructions.

JA9740273

(8) (a) Press, W. H.; Flannery, B. P.; Teukolsky, S. A.; Vetterling, W. T. *Numerical Recipies*; Cambridge University Press: Cambridge, 1986; pp 326−334. (b) Hustedt, E. J.; Smirnov, A. I.; Laub, C. F.; Cobb, C. E.; Beth, A. H. *Biophys. J.* **1997**, *74*, 1861−1877.

(9) The X-band simulations were insensitive to tensorial orientations: annealing runs which allowed these orientations to vary did not produce better fits (fit quality determined as described in the Supporting Information). Thus, with the exception of A_1 and A_2 of H^α, all hyperfine principal axis orientations were taken as collinear with the correspondingly indexed *g*-principal axis orientations. A_1 and A_2 of H^α were rotated by 30° from the corresponding *g*-principal axes to achieve better fits of 139.5 GHz EPR spectra reported previously.[2c] Each ^{13}C hyperfine value and associated uncertainty listed in Table 1 are the mean and 2 standard devations obtained from 60 annealing runs, with 2500 simulations calculated per run. The larger uncertainties in the ^{13}C A_1 and A_2 values reflect the broader range of convergence for these values in the simulated annealing runs. This broader range is expected for components whose splittings are not resolved in the EPR spectrum.

(10) The estimate of spin density was made using the equation[11]

$$A_{iso} = (Q^C_s + \sum_{j=1}^{3} Q^C_{CXj})\rho_i + \sum_{j=1}^{3} Q^C_{XjC}\rho_j$$

in which ρ_i is the spin density on the labeled carbon, ρ_j indexes spin density on adjacent atoms X_j, and the *Q* values are calculated spin polarization constants ($Q^C_s = -1.27$ mT, $Q^C_{CC'} = 1.44$ mT, $Q^C_{CH} = 1.95$ mT, $Q^C_{CO} = 1.77$ mT, $Q^C_{CC} = -1.39$ mT)[11,14] In addition, the unknown atom X in **3** has been assumed to have a *Q* value equal to that of oxygen, the spin density on hydrogen and on the unknown atom has been considered to be negligible, and the spin density on the 2′-carbon has been assumed to be −0.19, consistent with a typical allyl radical.[12]

(11) Karplus, M.; Fraenkel, G. K. *J. Chem. Phys.* **1962**, *35*, 1312−1323.

(12) Heller, C.; Cole, T. *J. Chem. Phys.* **1962**, *37*, 243−250.

(13) Camaioni, D. M.; Walter, H. F.; Jordan, J. E.; Pratt, D. W. *J. Am. Chem. Soc.* **1973**, *95*, 7978−7992.

(14) Das, M.; Fraenkel, G. *J. Chem. Phys.* **1965**, *42*, 1350.